PERFORMANCE COMPARISON OF STRUCTURAL DAMAGE DETECTION BASED ON FREQUENCY RESPONSE FUNCTION AND POWER SPECTRAL DENSITY

Mehrdad Hadizadeh-Bazaz, Ignacio-Javier Navarro y Víctor Yepes

Institute of Concrete Science and Technology (ICITECH), Universitat Politècnica de València. Av. dels Tarongers, 4D - 46022 Valencia (España).

Received: 20/dec/2021 • Reviewing: 20/dec/2021 • Accepted: 12/apr/2022 | DOI: https://doi.org/10.6036/10504

To cite this article:

HADIZADEH-BAZAZ, Mehrdad; NAVARRO, Ignacio-Javier; YEPES, Víctor. PERFORMANCE COMPARISON OF STRUCTURAL DAMAGE DETECTION BASED ON FREQUENCY RESPONSE FUNCTION AND POWER SPECTRAL DENSITY. DYNA September-October 2022. vol.97, n.5, pp. 493-500. DOI: https://doi.org/10.6036/10504

ABSTRACT:

Recent catastrophic events have aroused great interest in the scientific community regarding the evaluation and prediction of the structural response along the life cycle of infrastructures. Efforts are put into developing adequate health monitoring systems to help prevent future human life and economic losses. Here, two non-destructive damage detection methods are presented: the Frequency Response Function-based and the Spectral Density Function-based methods. The damage detection performance of both methods is compared through a particular case study, where different damage scenarios are analyzed in a 2D truss bridge. The reliability of each method is studied in terms of different prediction errors. Numerical results show that the PSD method for damage detection on a steel truss bridge structure provides more accurate and robust results when compared to that based on FRF.

Keywords: Structural Health Monitoring, Power Spectral Density Function, Frequency Response Function, Construction, Structures, Damage detection, Non-destructive

FUNDING

Grant PID2020-117056RB-I00 funded by MCIN/AEI/ 10.13039/501100011033 and by “ERDF A way of making Europe.”

1. - INTRODUCTION

The deterioration of the existing infrastructure has become a severe concern in developed countries. More than 30% of construction activity is currently related to the maintenance and refurbishment of damaged structures [1], revealing infrastructure maintenance and improvement as a significant source of long-term impacts [2]. As a result, while there is much interest in optimal structure design to reduce construction costs [3-5], structural deterioration mitigation has become a focus of many researchers aiming to provide optimal maintenance strategies to reduce life cycle costs [6-8].In such a context, information regarding damage detection and location has been crucial to increasing the accuracy of damage prediction methods assumed in maintenance optimization.

Actual trends in health monitoring of structures rely on the dynamic response variations associated with structural systems when deteriorated. Dynamic properties such as mass, stiffness, and damping may assist in identifying the location and extent of damage to structures according to non-destructive damage detection for numerical model updating in a structure [9-11]. Recently, some investigations have used or assessed the reliability and performance of dynamic techniques, either numerical or experimental, for non-destructive damage detection in steel, concrete, or composite structures. Some dynamics and vibration-based damage detection methods were evaluated by some researchers, such as: frequency response functions [12, 13], power spectral density [10,14], natural frequencies [15, 16], measured modal flexibility [17, 18], modal strain energy [19, 20], mode shapes [21]. Some researchers have used these methods individually or combined two or more [22-24]. Also, to compare the performance of these methods of identifying damage, some of these methods have been compared [25-28]. One of the most important ways to help engineers and experts choose and use the best method for the situation and type of structure is to compare the methods for diagnosing failure in different types and shapes of structures. Frequency response function (FRF) and power spectral density (PSD) methods are two common and popular methods based on the signal in damage detection. Comparing the performance and ability of these two methods in different conditions and structural shapes can be helpful information to researchers and engineers for selecting and using each of these methods in their studies.

In this regard, researchers on the FRF-based method followed some purposes. A structural model updating method based on FRF data and observed natural frequencies of the damaged structure was investigated according to the sensitivity equations to decrease model update nonlinearity. These sensitivity equations were also solved using Least Squares, non-linear [29], and linear [30]. The capacity of the FRF approach was evaluated in a model by simulating the mass modeling errors, and the stiffness degradation of structural parts was explored at the same time in the other case. It was shown in the research that the FRF method for updating findings was resistant to incompleteness, noise, and modeling error [31]. Also, a study examined the benefits of substituting unmeasured FRFs with EDTF in an accurate sensitivity equation. Extensive numerical experiments comparing the results of this technique with the dynamic expansion of observed mode shapes were done. Both techniques have advantages and disadvantages in mitigating the detrimental effects of incomplete measurement [32].

On the other hand, the PSD approach for damage detection was investigated in some publications. In a study, the pseudo excitation method (PEM) was used to get the dynamic response of structures and the power spectral density sensitivity to damage factors. This approach was used to obtain damage parameters repeatedly by the finite element model updating method in two numerical examples, including a flat-frame building and a 12-story shear building [33]. A unique algorithm and deterioration index for bridge concrete piers were developed. The power spectral density function was utilized to process structural responses. A damage index based on the least square distance was developed to diagnose the damage. The suggested algorithm and damage index may reliably identify and locate deterioration in bridge piers [34]. An Industrial Engineering researcher hypothesized that the method's accuracy is highly dependent on the damage degree. They tested the dependability using a massive dataset of 3500 incidents in a spring model with five degrees of structural integrity. When the structural integrity declined by 5%, the reliability plummeted to 95% [35].

To date, the performance of FRF and PSD methods has been evaluated and compared for a variety of structural systems and follows different approaches. For instance, some researchers compared the quasi-linear sensitivity of FRF with the derivation-based sensitivity of PSD to develop a sensitivity-based damage detection approach in a numerical frame and an experimental beam model [36]. Moreover, in the numerical models of plate and shell structures, updating frequency domain models using PSD to overcome the shortcomings of incomplete measurement allowed the sensitivity equation according to measured natural frequencies of a few lower modes [37]. Because the performance of frequency-based methods can differ in different types of structures and under different conditions, and in addition, construction, maintenance, and repair costs are essential for structures such as bridges, in this study, the performance of these two methods was compared with different approaches for detecting the extent, amount and location of damages on a numerical model of a two-dimensional steel truss bridge. For this purpose, these methods were compared by numerical analysis of the different elements of the structural system by using sensitivity equations. These equations were solved through the linear least square algorithm and model updating approach by monitoring changes in dynamic characteristics such as stiffness and mass of undamaged and damaged structural elements. The Closeness Index (CI), the Mean Size Error (MSE), and the Relative Error (RE) were used to evaluate the accuracy of predictions. Linearizing equations solve a non-linear relationship between structural parameters and observed response.

ISSN: 0012-7361 eISSN: 1989-1490 / DYNA Vol. 97 n.1 DOI: https://doi.org/10.6036/10504

2.- DAMAGE DETECTION METHODS

Generally, the FRF-based methods extract the structure data by exciting the degrees of freedom (DOF) and conducting measurements in the desired DOFs. The selection of these measurement locations has a significant impact on obtaining adequate damage detection results. The number of measurement locations is limited practically and economically [38,39]. On the other hand, the PSD- based method is a second-order transfer function by a sensitive and utterly non-linear function of structural parameters [33]. The following paragraphs present the mathematical background of each technique.

2.1.- FREQUENCY RESPONSE FUNCTION (FRF)

FRF is a transfer function (H(ω)) in the frequency domain that relates the displacement response of a structural system with its forces, as shown in Fig. 1. Such transfer function is, therefore, representative of the structural behavior of the structure under analysis [13]. The transfer function (H(ω)) varies due to changes in mass, damping, and stiffness, making FRF an ideal method for detecting damage. Some research has mentioned equations related to the FRF [22],[29-32], [37].

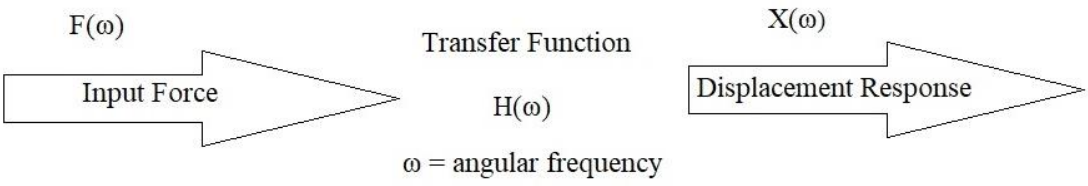

Fig. 1. Transfer Function of FRF with Input Force to Displacement Response

The analytical equation defining the FRF can be derived from the equation of motion of a structural system with n degrees of freedom:

$$\boldsymbol{M}\ddot{\boldsymbol{x}}(\boldsymbol{t}) + \boldsymbol{C}\dot{\boldsymbol{x}}(\boldsymbol{t}) + \boldsymbol{K}\boldsymbol{x}(\boldsymbol{t}) = \boldsymbol{f}(\boldsymbol{t}) \quad (\mathbf{1})$$

Where *M*, *C,* and *K* represent the structural system's mass, damping, and stiffness matrices, respectively, *f(t)* represents the input force vector applied to the system, and *x(t)* is the nodal displacement vector. Assuming that the force input is harmonic, exciting force *f(t)* and the resulting displacement *x(t)* can be expressed as:

$$f(t) = F(\omega)e^{i\omega t} \quad (2)$$

$$x(t) = X(\omega)e^{i\omega t} \quad (3)$$

Where *F(ω)* and *X(ω)* are the displacements and the applied force expressed in the frequency domain, respectively, and *ω* is the excitation frequency of the structure. Substituting Eqs. (2)-(3) in Eq. (1):

$$[-M\omega^2 - i\omega C + K]X(\omega) = F(\omega) \quad (4)$$

The equation can be rewritten to derive the analytical expression for the FRF transfer matrix *H(ω)*:

$$H(\omega) = [-M\omega^2 + i\omega C + K]^{-1} \quad (5)$$

A formula for changing the transfer matrix when the structural system is damaged from the above equations is given below. To do so, on the one hand, we shall consider that the structural response $X_i(\omega)$ of a particular degree of freedom *i* of the system when a unitary harmonic load $F_l(\omega)$ is applied can be expressed as:

$$X_i(\omega) = H_{il}(\omega)F_l(\omega) = H_{il}(\omega) \quad (6)$$

Where $F_l(\omega)$ is a vector with every component equal to zero except for the component *l*, which is equal to one, on the other hand, the structural response of a system can also be obtained as a linear superposition of modes:

$$X = \sum_{r=1}^{n} \varphi_r q_r \quad (7)$$

ISSN: 0012-7361 eISSN: 1989-1490 / DYNA Vol. 97 n.1 DOI: https://doi.org/10.6036/10504

Where φ is, the mode shape matrix and q represent the modal coordinate matrix. Thus, Eq. (1) can be rewritten as:

$$M\varphi_r\ddot{q}_r + C\varphi_r\dot{q}_r + K\varphi_r q_r = f(\omega) \quad (8)$$

Multiplying both sides of Eq. (1) by the transposed mode shape matrix, we get:

$$(-\omega^2\varphi_r^T M\Phi_r + i\omega\varphi_r^T C\Phi_r + \varphi_r^T K\Phi_r)\bar{q}_r = \varphi_r^T F(\omega)e^{i\omega t} \quad (9)$$

This equation can be simplified into:

$$(-\omega^2 M_r + i\omega C_r + K_r)\bar{q}_r = \varphi_r^T F(\omega) \quad (10)$$

The relation between the mass, damping, and stiffness matrices can also be expressed in modal terms as:

$$C_r = 2\xi_r\omega_r M_r \quad (11)$$

$$K_r = M_r\omega_r^2 \quad (12)$$

Consequently, we can rewrite Eq. (9) into:

$$(-\omega^2 + i\omega(2\xi_r\omega_r) + \omega_r^2)\bar{q}_r = \varphi_r^T F(\omega) = \varphi_{lr} \quad (13)$$

By placing Eq. (12) into Eq. (6), we get:

$$H_{il} = \sum_{r=1}^{n}\frac{\varphi_{ir}\varphi_{lr}}{\omega_r^2-\omega^2+2i\omega\xi_r\omega_r} \quad (14)$$

Where φ_r represents the structural mode, ω_r *is* the natural frequency, and ξ_r is the modal damping. In fact, in the above equation, H_{il} is the displacement of the degree of freedom *i* when the unit load excites the degree of freedom *l*. When the structure has deteriorated, the modal response of the system changes as:

$$\varphi_{rdi} = \varphi_{ri} + \delta\varphi_{ri} \quad (15)$$

Where φ_{rdi} represents the mode shape of the damaged structure for the degree of freedom *i*, and $\delta\varphi_{ri}$ stands for its deformation rate. Therefore, Eq. (14) can be rewritten for a damaged structure as:

$$H_{ild} \cong \sum_{r=1}^{nm}\frac{\varphi_{ird}\varphi_{lrd}}{\omega_{rd}^2-\omega^2+2i\omega\xi_{rd}\omega_{rd}} + \sum_{r=nm+1}^{nm}\frac{\varphi_{ir}\varphi_{lr}}{\omega_r^2-\omega^2+2i\omega\xi_r\omega_r} \quad (16)$$

Eq. (16) approximation is not unrealistic because natural frequencies can be obtained with high accuracy. The second part of the Eq. (16) deals with the unmeasured portion of natural frequencies and damping coefficients and reduces the effect of incomplete measurement. By inserting Eq. (15) into the first part of Eq. (16), it is derived that:

$$H_{ild} \cong \widetilde{H}_{il} + \Delta H_{il} = \sum_{r=1}^{nm}\frac{\varphi_{ir}\varphi_{lr}}{\omega_{rd}^2-\omega^2+2i\omega\xi_{rd}\omega_{rd}} + \sum_{r=nm+1}^{n}\frac{\varphi_{ir}\varphi_{lr}}{\omega_r^2-\omega^2+2i\omega\xi_r\omega_r} + \sum_{r=1}^{nm}\frac{\varphi_{ir}\delta\varphi_{lr}}{\omega_{rd}^2-\omega^2+2i\omega\xi_{rd}\omega_{rd}} + \sum_{r=1}^{nm}\frac{\delta\varphi_{ir}\varphi_{lr}}{\omega_{rd}^2-\omega^2+2i\omega\xi_{rd}\omega_{rd}} \quad (17)$$

The modal deformation rate $\delta\varphi_{lr}$ can be obtained by:

$$\delta\varphi_{lr} \cong \sum_{q=1}^{n}\alpha_{rq}\varphi_{lq} \quad (18)$$

Where *α* can be calculated as follows, by multiplying both sides of Eq. (12) by the mode matrix φ_q and deriving it, we get:

$$\delta K\varphi_q + K\delta\varphi_q = \delta M\varphi_q\omega_q^2 + M\delta\varphi_q\omega_q^2 + 2M\varphi_q\omega_q\delta\omega \quad (19)$$

Sorting Eq. (19) appropriately, the value of *α* can obtain as:

$$\begin{cases}\alpha_{rq} = \dfrac{\varphi_q^T(\delta K-\omega^2\delta M)\varphi_r}{(\omega_r^2-\omega_q^2)} & for \quad q \neq r \\ \alpha_{rq} = -\dfrac{\varphi_q^T(\delta M)\varphi_r}{2} & for \quad q = r\end{cases} \quad (20)$$

ISSN: 0012-7361 eISSN: 1989-1490 / DYNA Vol. 97 n.1 DOI: https://doi.org/10.6036/10504

Since the mass changes due to deterioration are usually minor compared to the changes in stiffness, changes in mass are neglected when deriving the above equations. Taking this assumption into account (*δM= 0),* we can rewrite the second term of Eq. (17), namely ΔH_{il} as:

$$\Delta H_{il} = \sum_{r=1}^{nm} \frac{\varphi_{ir}\delta\varphi_{lr}}{\omega_{rd}^2-\omega^2+2i\omega\xi_{rd}\omega_{rd}} + \sum_{r=1}^{nm} \frac{\delta\varphi_{ir}\varphi_{lr}}{\omega_{rd}^2-\omega^2+2i\omega\xi_{rd}\omega_{rd}} =$$
$$\sum_{r=1}^{nm}\sum_{q=1}^{n} \frac{\varphi_{ir}(\varphi_q^T\delta K\varphi_i)\varphi_{lq}}{(\omega_{rd}^2-\omega^2+2i\omega\xi_{rd}\omega_{rd})(\omega_i^2-\omega_q^2)} + \sum_{r=1}^{nm}\sum_{q=1}^{n} \frac{(\varphi_q^T\delta K\varphi_i)\varphi_{iq}\varphi_{lr}}{(\omega_{rd}^2-\omega^2+2i\omega\xi_{rd}\omega_{rd})(\omega_i^2-\omega_q^2)} \quad (21)$$

Defined the stiffness matrix of healthy (K_h) and damaged (K_d) structure as follows:

$$K_h = APA^T \quad (22)$$

$$K_d = K_h + \delta K = A(P+\delta P)A^T \quad (23)$$

The matrix *A* is a function of the geometric properties of the elements, and the diagonal matrix *P* contains mechanical properties (like bending and axial stiffness). If we consider that the stiffness changes are reflected in changes in the *P* matrix, we will have:

$$\delta K = A\delta PA^T \quad (24)$$

Finally, if we place Eq. (24) into Eq. (21), we get an analytical expression for the variations in the transfer matrix due to deterioration of the structural system:

$$\Delta H_{il} = [\sum_{r=1}^{nm}\sum_{q=1}^{n} \frac{\varphi_{ir}(\varphi_q^T\, Adiag(A^T\varphi_r))\varphi_{lq}}{(\omega_{rd}^2-\omega^2+2i\omega\xi_{rd}\omega_{rd})(\omega_i^2-\omega_q^2)} + \sum_{r=1}^{nm}\sum_{q=1}^{n} \frac{\varphi_{iq}(\varphi_q^T\, Adiag(A^T\varphi_r))\varphi_{lr}}{(\omega_{rd}^2-\omega^2+2i\omega\xi_{rd}\omega_{rd})(\omega_i^2-\omega_q^2)}]\delta P = S_H\delta P \quad (25)$$

2.2.- POWER SPECTRAL DENSITY (PSD)

FRF methods rely on an adequate monitorization of the structure to be analyzed. Given that it is neither practical nor economical to excite and monitor every degree of freedom of a structure, PSD-based methods are recognized as an alternative to overcome such limitations of FRF damage detection methods. Based on the equations in random vibrations, the spectral density function of a structural response can be expressed as following equations according to some research on the PSD method [33], [36,37].

$$S_{XX} = HS_{ff}H^T \quad (26)$$

S_{XX} is the output response PSD function, S_{ff} is the input response PSD function, and *H* is the transference function presented in the previous section. Taking into account Eq. (17), S_{XX} can be obtained for a damaged structural system as:

$$S_{xxd} \cong \tilde{H}S_{ff}\tilde{H}^T + \Delta HS_{ff}\tilde{H}^T + \tilde{H}S_{ff}\Delta H^T + \Delta H^TS_{ff}\Delta H^T \quad (27)$$

From the above, it can be derived that the variation of the output response PSD function when the structural system under analysis is damaged can be expressed as follows:

$$\Delta S_{xx} = S_{xxd} - \tilde{H}S_{ff}\tilde{H}^T = \Delta HS_{ff}\tilde{H}^T + \tilde{H}S_{ff}\Delta H^T \quad (28)$$

Assuming the value of *ΔH* deduced in Eq. (25), we can rewrite Eq. (28) as:

$$\Delta S_{xx} \cong \left[S_HS_{ff}\tilde{H}^T + \tilde{H}S_{ff}S_H^T\right]\delta P \quad (29)$$

Taking into consideration the analytical expression of S_H presented in Eq. (25), we can formulate the final sensitivity equation as:

$$S_s = S_HS_{ff}\tilde{H}^T + \tilde{H}S_{ff}S_H^T =$$
$$[\sum_{r=1}^{nm}\sum_{q=1}^{n} \frac{\varphi_{ir}(\varphi_q^T\, Adiag(A^T\varphi_r))\varphi_{lq}}{(\omega_{rd}^2-\omega^2+2i\omega\xi_{rd}\omega_{rd})(\omega_i^2-\omega_q^2)} + \sum_{r=1}^{nm}\sum_{q=1}^{n} \frac{\varphi_{iq}(\varphi_q^T\, Adiag(A^T\varphi_r))\Phi_{lr}}{(\omega_{rd}^2-\omega^2+2i\omega\xi_{rd}\omega_{rd})(\omega_i^2-\omega_q^2)}]\, S_{ff}[\sum_{r=1}^{nm} \frac{\varphi_{ir}\varphi_{lr}}{\omega_{rd}^2-\omega^2+2i\omega\xi_{rd}\omega_{rd}} +$$

ISSN: 0012-7361 eISSN: 1989-1490 / DYNA Vol. 97 n.1 DOI: https://doi.org/10.6036/10504

$$\sum_{r=nm+1}^{n}\frac{\varphi_{ir}\varphi_{lr}}{\omega_d^2-\omega^2+2i\omega\xi_d\omega_d}]^T+[\sum_{r=1}^{nm}\frac{\varphi_{ir}\varphi_{lr}}{\omega_{rd}^2-\omega^2+2i\omega\xi_{rd}\omega_{rd}}+$$
$$\sum_{r=nm+1}^{n}\frac{\varphi_{ir}\varphi_{lr}}{\omega_d^2-\omega^2+2i\omega\xi_d\omega_d}]S_{ff}[\sum_{r=1}^{nm}\sum_{q=1}^{n}\frac{\varphi_{ir}(\varphi_q^T\,Adiag(A^T\varphi_r))\varphi_{lq}}{(\omega_{rd}^2-\omega^2+2i\omega\xi_{rd}\omega_{rd})(\omega_i^2-\omega_q^2)}+\sum_{r=1}^{nm}\sum_{q=1}^{n}\frac{\varphi_{iq}(\varphi_q^T\,Adiag(A^T\varphi_r))\varphi_{lr}}{(\omega_{rd}^2-\omega^2+2i\omega\xi_{rd}\omega_{rd})(\omega_i^2-\omega_q^2)}]^T \quad (30)$$

Finally, the PSD function can be formulated as:

$$\Delta S_{xx}\cong S_s\delta P \qquad (31)$$

Where δP represents the structural changes in the system's stiffness resulting from deterioration, by solving Eq. (31), the changes in stiffness for damaged structures can be calculated by comparison with the response of the undamaged structure using the least square method. This equation is solved through iteration. The stiffness matrix of the undamaged structure is updated according to the calculated stiffness change, thus modifying the PSD in every iteration and model updating and cause made more accurate damage prediction. The difference obtained between the damaged and the undamaged structure is as much as the damage aimed to evaluate.

3.- NUMERICAL EXAMPLE

The presented damage detection algorithm was applied to an eight-bay truss structure with the geometry, connectivity, and active DOFs shown in Fig. 2. Each span is 1.5m for a total of 12m. The structure is modeled numerically using the finite element method with structural elements stressed with axial loads. Truss elements are made from steel with Young's modulus of 200Gpa, a mass density of 7300 kg/m3. The structure consists of 35 steel elements connected by 16 nodes. The cross-sectional areas for elements 1–8 (top chord), 9–16 (Bottom chord), 17–23 (vertical), and 24–35 (Diagonal bracing) are respectively 1.8, 1.5, 1.0, and 1.2 (cm²). Considered 29 active DOFs, with 2 degrees of freedom per node (Fig. 2(b)). Nodes can only move horizontally and vertically except for node 1, where no displacement is allowed, and node 9, where only horizontal motions are allowed. Every system element has steel material attributes.

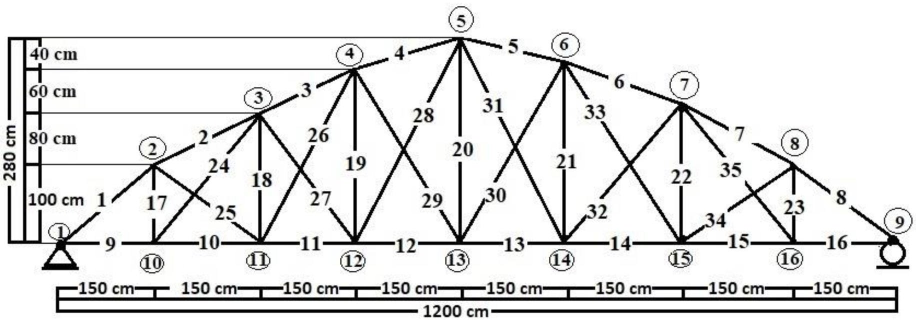

(a)

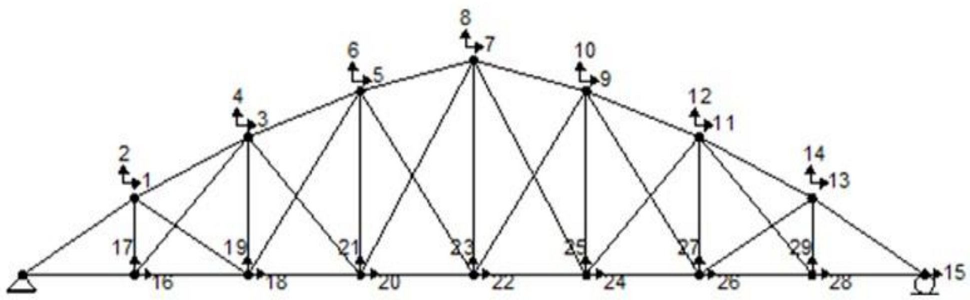

(b)

Fig. 2. The trust model information: (a) Geometry; (b) Active degree of freedom direction

In this model, loads are applied at the structure's nodes so that only axial forces act on each element. Therefore, the structure's stiffness is given by the axial stiffness of the truss elements, defined by their cross-sectional area and the modulus of elasticity of the assumed material. A decrease in the steel modulus of elasticity shows how the steel will degrade since these values are assumed to remain constant.

ISSN: 0012-7361 eISSN: 1989-1490 / DYNA Vol. 97 n.1 DOI: https://doi.org/10.6036/10504

The injury scenarios considered to determine the differences in the accuracy of the FRF and PSD damage detection methods are presented in Table 1 below. In order to identify more groups of possible damage to the structure, it is assumed that the damages can differ in each scenario.

Damage Mode	Element Number	Percentage of Damage
Scenario 1	5	30
	14	50
Scenario 2	14	40
	16	50
	23	60
Scenario 3	3	30
	11	30
	32	30
	35	30
Scenario 4	7	30
	19	40
	27	50
Scenario 5	2	30
	9	40
	13	50
	29	40
	33	30
Scenario 6	10	30
	17	30
	26	30
	34	30
Scenario 7	6	40
	20	70
Scenario 8	8	30
	24	40
	31	60

Table 1. Damage scenarios considered

Damages in different structures can appear in different ways, which in concrete structures are usually on the surface and deep cracks on the structural elements. In steel structures, it appears as corrosion and rust in coastal environments. It shall be noted that there are not all the damage types that may appear on a structure. However, for simplicity and interpretation of the results, the actual comparative research is focused solely on deterioration caused naturally. The truss structure is modeled numerically using the finite element method by the Software.

3.1.- CALIBRATION OF THE NUMERICAL MODEL

Excitation frequency ranges, selection, number and location of measurements, and simulation DOFs all play a role in the success of a model updating scheme using FRF and PSD data. For this purpose, selected a scenario of damage in Table 1 and used different DOFs set groups in Table 2 as base data for assessment by one of these methods. In this study, for selecting suitable DOFs set as the base data of the measurement locations and excitation loads data for analysis of the eight damage prediction scenarios, some groupsets were considered in Table 2 mentioned four of them as samples. The rotating DOFs were not subjected to stimulation or measurement. Each set was analyzed by the FRF method to predict damage percent in the structure for the first scenario from Table 1.

ISSN: 0012-7361 eISSN: 1989-1490 / DYNA Vol. 97 n.1 DOI: https://doi.org/10.6036/10504

Sets	Measurements DOFs	Stimulations DOFs	Test according to scenario 1		
			Predicted damage (%)		RMSE*
			Element 5	Element 14	
1	3-9-14-22-24	8-11-13-17-18-25	-5	25	30.4%
2	4-11-13-21-27	6-7-12-17-18-23	20	-5	39.5%
3	4-7-10-25-27	4-7-11-16-20-25	-8	-8	49.0%
4	9-13-15-17-19	7-9-11-14-17-18-27-28	40	48	7.2%
*RMSE: The Root Mean Square Error					

Table 2. The measurements and stimulation DOFs set

Table 2 shows the RMSE for scenario1 through the fourth set of the measurements and stimulations DOFs set are less than other sets. So, as base data to analyses in software for damage prediction by FRF and PSD methods for the eight damage scenarios of Table 1, the DOFs 9, 13, 15, 17, and 19 are selected as the measurement locations, and DOFs 7, 9, 11, 23, 25, and 29 as excitation loads were assumed.
Due to imperfections such as ambient noise, FE modeling mistakes, and measurement errors, inevitable errors, and variances in finite element model update results are inevitable. To test the suggested method's resilience against measurement error, 10% random error is considered for each FRF and PSD method.

For scenario 1, Figure 3 illustrates the comparison of the FRFs of damaged and undamaged buildings determined from vibration testing.

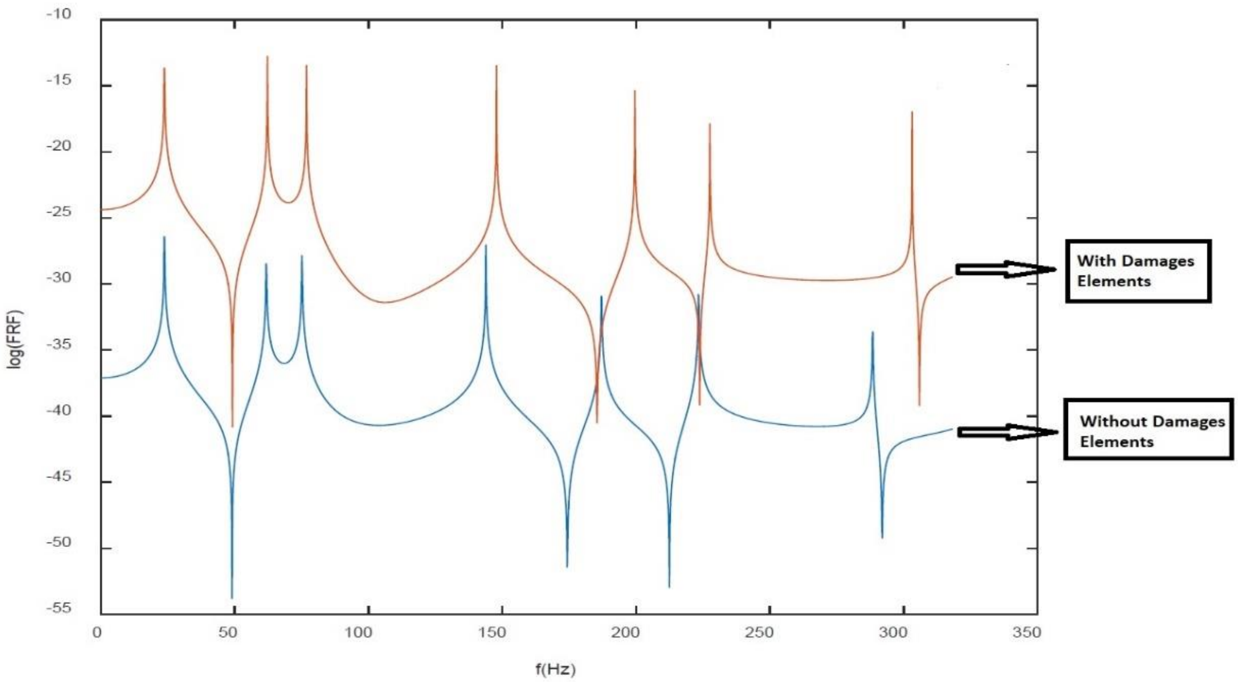

Fig. 3. Comparison of the FRFs according to the damaged and undamaged elements for the scenario1

As Fig. 3, responses frequency by the FRF for undamaged and damaged structures was used to determine the structure damage situation. The diagram also shows that the first scenario using the FRF method at low frequencies is almost ineffective and gradually increases with increasing frequency at the selected excitation fourth set in Table 2, which indicates an increase in damage and a decrease in stiffness of some elements. The FRF data for the damaged structure was moved from the undamaged structure due to the structure's loss of stiffness due to the damage.

ISSN: 0012-7361 eISSN: 1989-1490 / DYNA Vol. 97 n.1 DOI: https://doi.org/10.6036/10504

4.- RESULTS AND DISCUSSION

Each damage detection method, such as FRF and PSD Function, was compared with its anticipated damage rate on software and the actual damage rate in each damaged situation in Table 1 for comparison and assessment using MATLAB software and the formulae and equations.

As shown in Figure 4, the damage prediction results for each of the eight damaged situations in Table 1 are shown in a chart bar for each technique in Table 1.

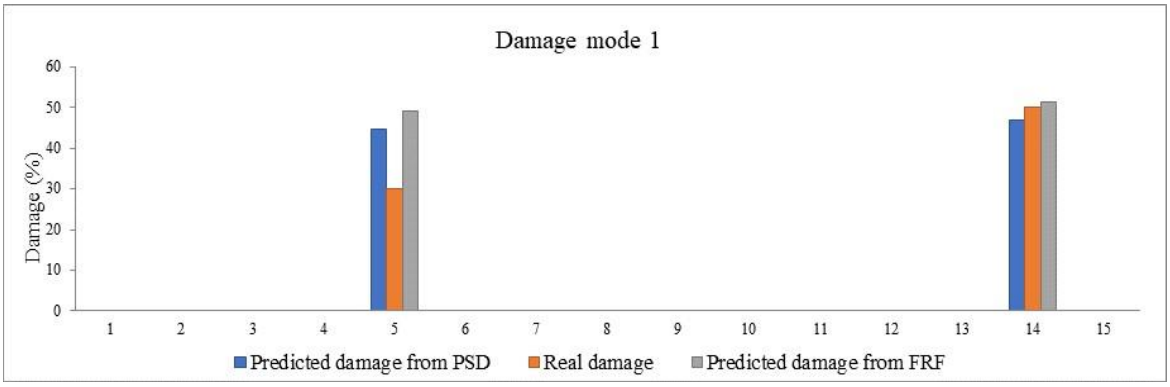

(a) Scenario 1

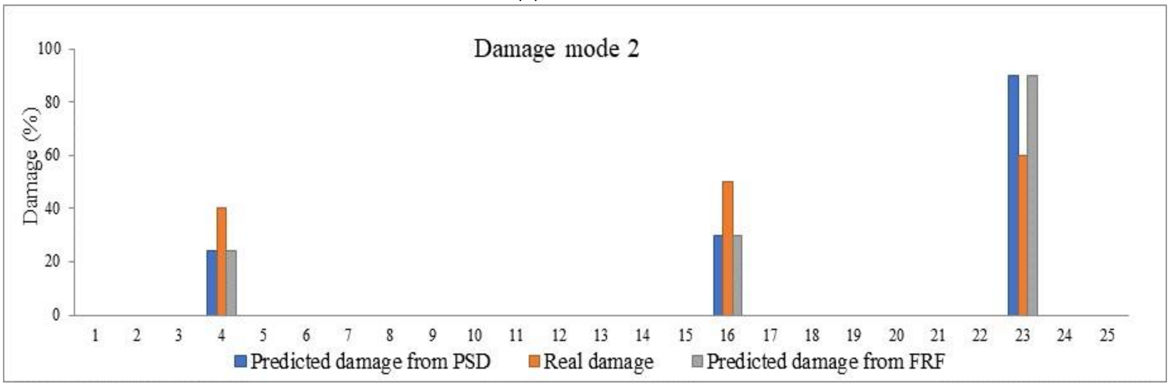

(b) Scenario 2

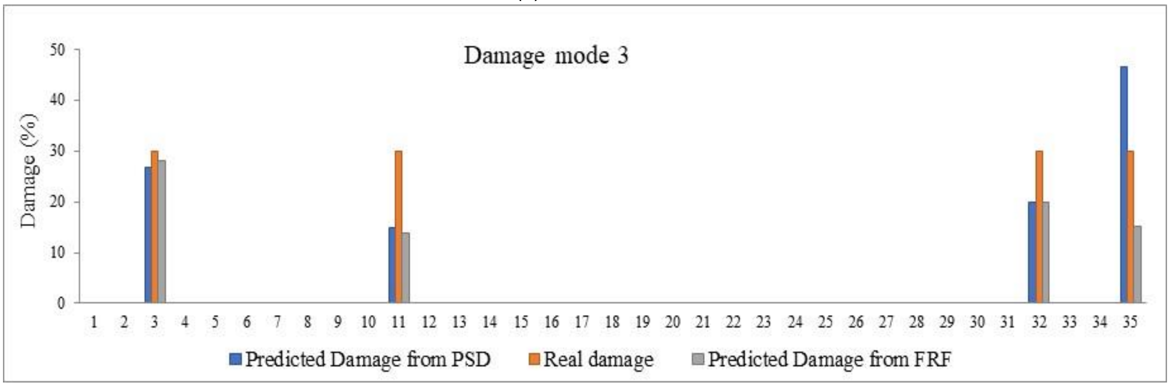

(c) Scenario 3

ISSN: 0012-7361 eISSN: 1989-1490 / DYNA Vol. 97 n.1 DOI: https://doi.org/10.6036/10504

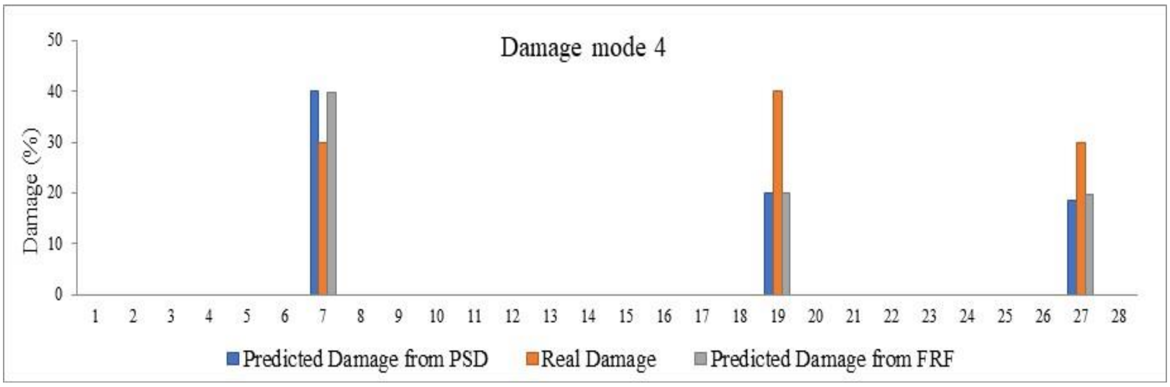

(d) Scenario 4

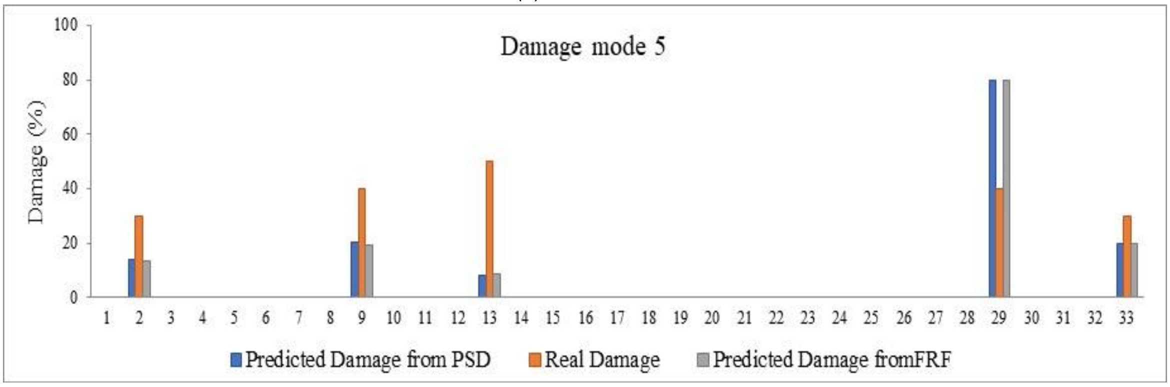

(e) Scenario 5

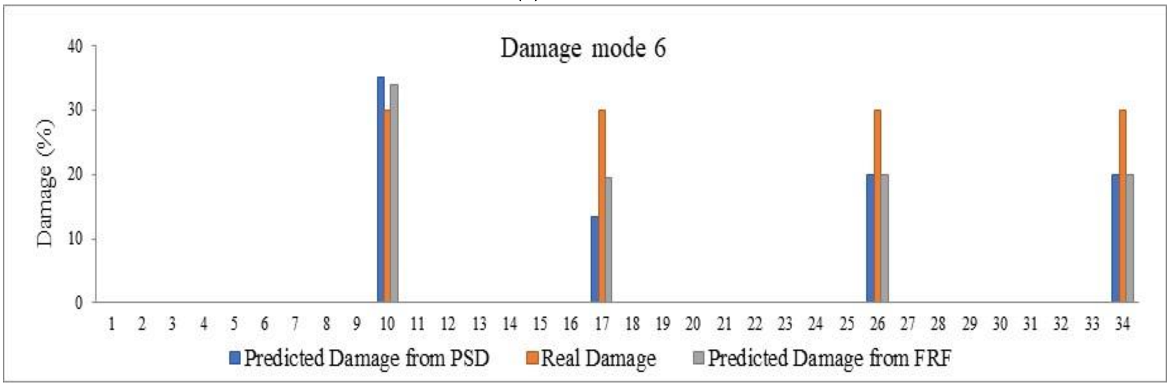

(f) Scenario 6

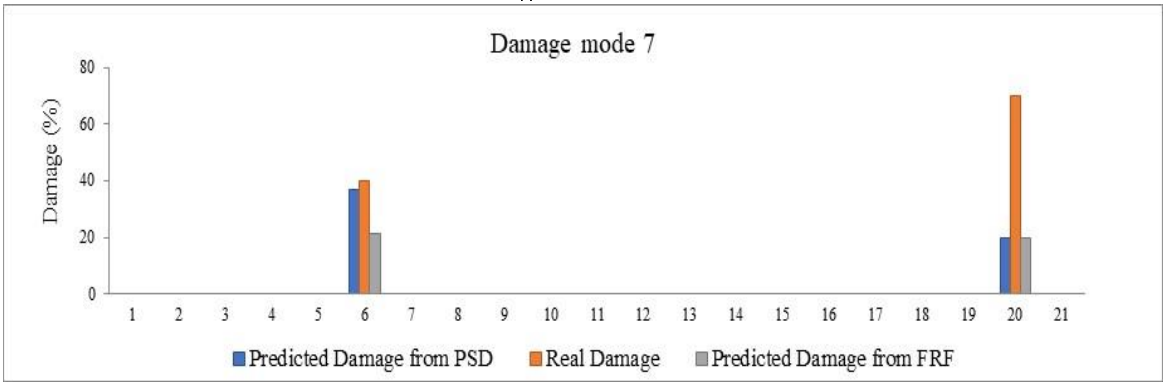

(g) Scenario 7

ISSN: 0012-7361 eISSN: 1989-1490 / DYNA Vol. 97 n.1 DOI: https://doi.org/10.6036/10504

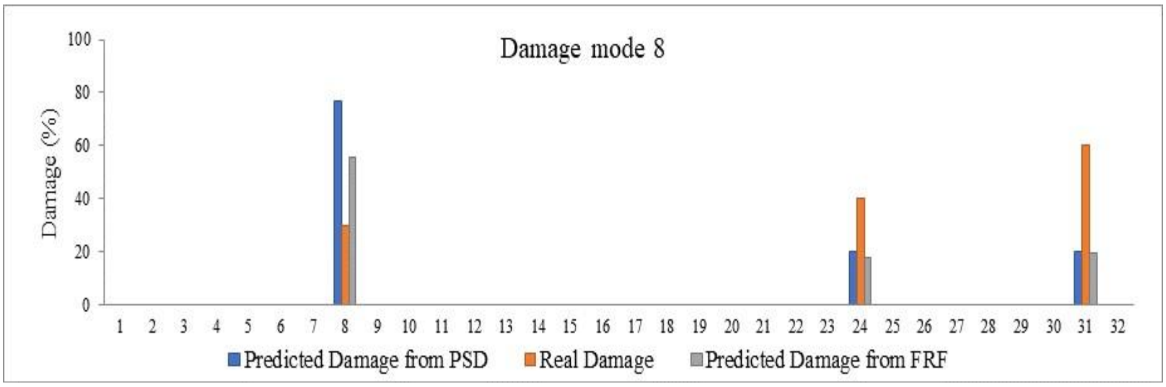

(h) Scenario 8

Fig. 4 Comparison of The Predicted Damage with FRF and PSD methods and for different scenarios

In Figure 4, the teal damages are damaged elements from scenarios considered in Table 1 as actual damages. After analysis, the percentage of predicted damages by FRF and PSD method for each scenario is compared according to the same conditions.

Three alternative error assessments are examined to quantify the quality of the predictions, namely the Closeness Index (CI), the Mean Size Error (MSE), and the Relative Error (RE) [29].
The Closeness Index indicates how close the predicted amount of damage has relation to the actual damage of the structure:

$$CI = 1 - \frac{|\delta p_p - \delta p_a|}{|\delta p_a|} \qquad (32)$$

Where δP_P is the predicted damage, and δP_a is the actual damage in each of the considered damage scenarios. A value of the closeness index equal to 1 means an exact fit of the prediction. The *MSE* is the average of the absolute differences between the actual and the predicted damage:

$$MSE = \frac{1}{n}\sum_{i=1}^{n} |\delta p_{ai} - \delta p_{pi}| \qquad (33)$$

The *n* denotes the number of structural elements.
The Relative Error Index of a prediction shall be calculated as:

$$RE = \frac{\sum_{i=1}^{n}|\delta p_{ai}| - \sum_{i=1}^{ni}|\delta p_{ai}|}{\sum_{i=1}^{ni}|\delta p_{ai}|} \qquad (34)$$

Fig. 5 shows the results of the abovementioned error indices for the two prediction methods. It can be observed that, in general, PSD shows better *CI* results, with prediction errors ranging from 0.36 to 0.73. As far as *MSE* is concerned, for the damage scenario 2, PSD presents slightly worse results than FRF. It shall be noticed that the error regarding damage scenario 5 is, as in the case of *CI* evaluation, the scenario with the highest error for both detection methods. This equation can attribute to the model's numerical errors rather than the goodness of predictions. At last, the *RE* results do not show sensitivity to the damage scenario under study, presenting prediction errors that do not exceed 0.63 in the worst case. In general, PSD-based predictions result in lower *RE* values than those derived from the FRF method.

ISSN: 0012-7361 eISSN: 1989-1490 / DYNA Vol. 97 n.1 DOI: https://doi.org/10.6036/10504

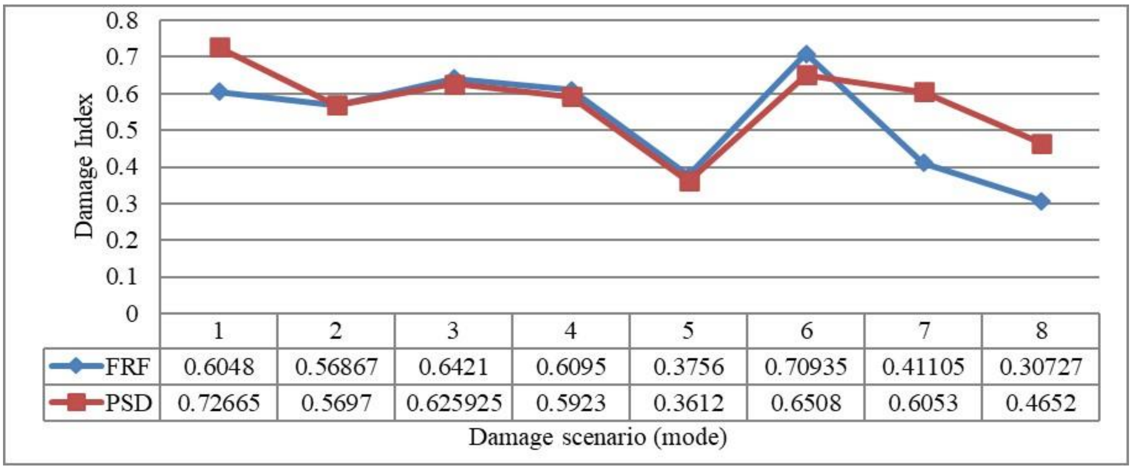

(a) Closeness Index

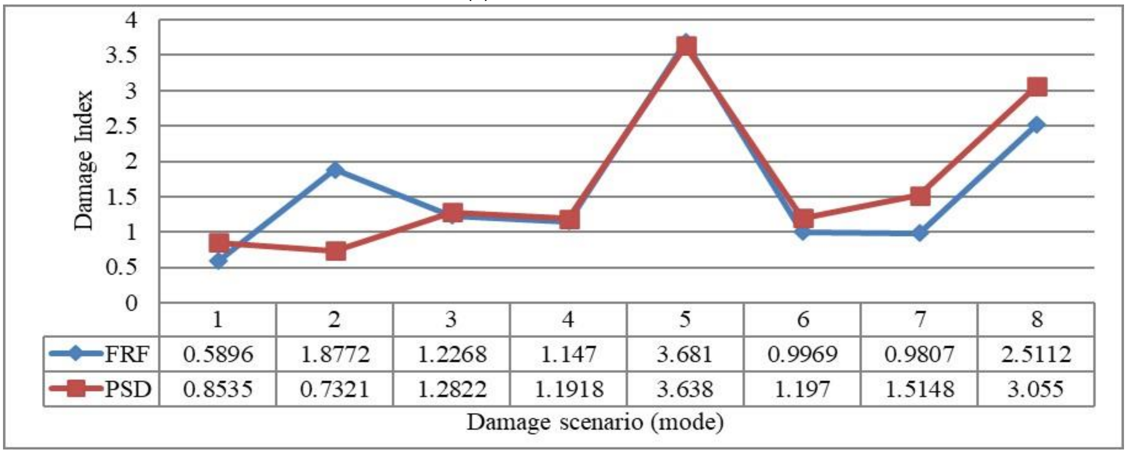

(b) Mean Size Error

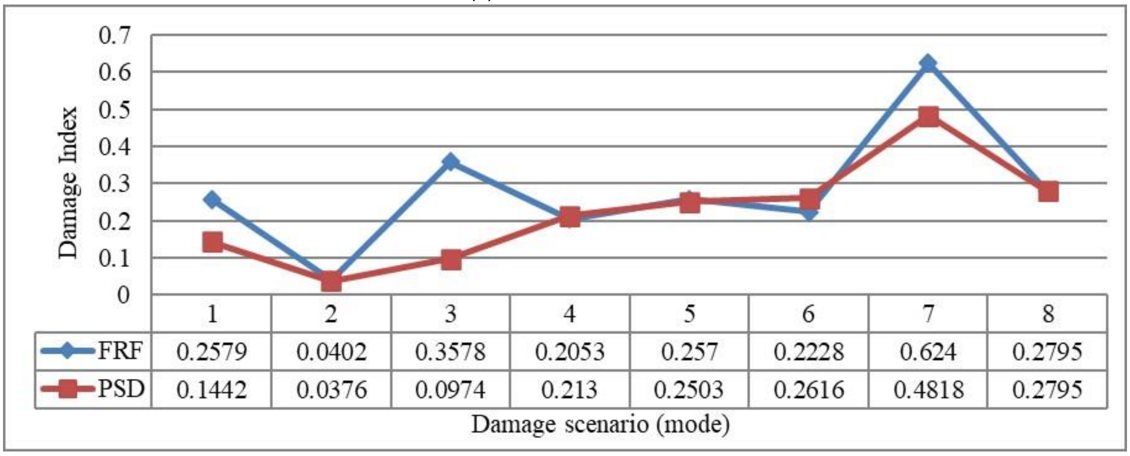

(c) Relative Error

Fig. 5 Error Indices results for The Two methods of Damage Detection for the eight scenarios

The average achieved for PSD and FRF in the three error metrics studied here is shown in Table 3. In addition, for each detection technique, the interquartile range (IQR) was determined to define the statistical dispersion of the data.

ISSN: 0012-7361 eISSN: 1989-1490 / DYNA Vol. 97 n.1 DOI: https://doi.org/10.6036/10504

Methods	CI		MSE		RE	
	Average	IQR	Average	IQR	Average	IQR
FRF	0.529	0.355	1.351	2.644	0.281	0.433
PSD	0.575	0.303	1.246	2.30	0.221	0.352
*IQR: The interquartile range measurements						

Table 3. Summary of Average Errors and IQR

In comparison to FRF, PSD performs better in terms of average results for each of the three error measures evaluated, with an average CI closer to one and average MSE and RE values closer to zero. In each of the three error measurements, PSD displays IQR values that are lower than those obtained using the FRF approach. According to the findings obtained for the case study under consideration, PSD outperformed FRF and provides more trustworthy damage prediction predictions.

As previously investigated based on numerical results, FRF and PSD methods have been compared on a numerical model of a 2D one story by one bay steel frame and a laboratory concrete beam vibration test [36]. The comparison result with the FRF made only on two groups of damage scenarios based on sensitivity equations showed the PSD method's performance in detecting the location and extent of damages [36].

However, the research analysis results on the steel truss bridge almost confirmed some of the other results on a steel one-bay frame and the concrete beam [36], and also some comparison mentions on a plate and a shall shape structure model without numerical analysis result through the FRF method [37], show that the PSD method is more sensitive than FRF method in structural parameter changes, especially in the natural frequency range. While in other structural model shapes, for the low-frequency range and low or noise-free conditions, the FRF method was more accurate than PSD, this study on truss shape shows that the PSD method also has an almost more accurate and reliable performance in the low and medium-frequency ranges as calculated by software analyses. Thus, future studies are required to identify what method, PSD or FRF, performs best in detecting damages for different types of structural systems, materials, or structural variables.

5.- CONCLUSIONS

Because damage detection in infrastructures such as bridges is critical, the current research examines the performance and accuracy of two dynamic and non-destructive approaches based on FRF and PSD in determining the amount of damage in the structural elements of a truss steel bridge. This comparison was made under the same conditions and with the DOFs' excitation and measurement properties. The quantified damages in this truss were predicted by analyzing these methods according to their solutions to sensitivity equations through the linear least-square algorithm and model updating approach. For analyzing each method, changes in dynamic characteristics such as stiffness and mass in undamaged and damaged structural elements were monitored. This issue is solved by linearizing equations, which is an inverse problem since the link between structural parameters and observed response is intrinsically non-linear. For a more accurate evaluation, The error Indices results were calculated. In particular, errors obtained with PSD-based prediction show average CI and MSE errors that were 8.5% lower than those obtained with FRF based and 27% lower when considering RE. Regarding statistical dispersion, PSD results in IQR values between 14% and 23% lower than the dispersion observed when applying the FRF method.
In summary, since comparing methods for detecting and predicting structural damage can show each method's superiority or lack of superiority depending on the conditions and structure, it is best to compare their performance. To improve the comparability of these methods, they should be tested on a variety of structures, conditions, and materials. For the particular case study analyzed here, comparing the numerical results of the two methods revealed that the PSD is more accurate in predicting and diagnosing structural element damage in a metal truss structure with oblique elements than FRF.

REFERENCES

[1] Gil Benso E, Vercher Sanchis JM, Mas Tomas MD, Fenollosa Forner EJ. "Seguridad remanente a flexión en forjados con corrosión en las viguetas". *Informes de la Construcción.* 2015. Vol. 67(537). p.e054. DOI: http://dx.doi.org/10.3989/ic.13.084

[2] Sierra LA, Pellicer E, Yepes V. “Method for estimating the social sustainability of infrastructure projects”. *Environmental Impact Assessment Review*. 2017. Vol. 65. p.41-53. DOI: https://doi.org/10.1016/j.eiar.2017.02.004

[3] Paya-Zaforteza I, Yepes V, González-Vidosa F, Hospitaler A. “On the Weibull cost estimation of building frames designed by simulated annealing”. *Meccanica.* February 2010. Vol. 45(5). p.693-704. DOI: https://doi.org/10.1007/s11012-010-9285-0.

[4] García-Segura T, Yepes V, Frangopol DM. “Multi-objective design of post-tensioned concrete road bridges using artificial neural networks”. *Structural and Multidisciplinary Optimization*. February 2017. Vol. 56(1). p.139-150. DOI: https://doi.org/10.1007/s00158-017-1653-0

[5] Penadés-Plà V, Martí JV, García-Segura T, Yepes V. “Life-cycle assessment: A comparison between two optimal post-tensioned concrete box-girder road bridges”. *Sustainability*. October 2017. Vol. 9(10). p.1864. DOI: https://doi.org/10.3390/su9101864

[6] Navarro IJ, Marti JV, Yepes V. “Reliability-based maintenance optimization of corrosion preventive designs under a life cycle perspective”. *Environmental Impact Assessment Review.* January 2019. Vol. 74. p.23-34. DOI: https://doi.org/10.1016/j.eiar.2018.10.001

[7] Sajedi S, Huang Q. “Reliability-based life-cycle-cost comparison of different corrosion management strategies”. *Engineering Structures*. May 2019. Vol. 186. p.52-63. DOI: https://doi.org/10.1016/j.engstruct.2019.02.018

[8] Navarro IJ, Yepes V, Martí JV. “Life cycle cost assessment of preventive strategies applied to prestressed concrete bridges exposed to chlorides”. *Sustainability*. March 2018. Vol. 10(3). p.845. DOI: https://doi.org/10.3390/su10030845

[9] Pedram M, Esfandiari A, Khedmati MR. “Finite element model updating using strain-based power spectral density for damage detection”. *Structural Control and Health Monitoring*. November 2016. Vol. 23(11). p.1314-33. DOI: https://doi.org/10.1002/stc.1833

[10] Li J, Hao H, Xia Y, Zhu HP. “Damage assessment of shear connectors with vibration measurements and power spectral density transmissibility”. *Structural engineering and mechanics*: *An international journal*. 2015. Vol. 54(2). p.257-89. DOI: http://dx.doi.org/10.12989/sem.2015.54.2.257.

[11] Pehlivan H. Frequency analysis of GPS data for structural health monitoring observations. *Structural Engineering and Mechanics*. January 2018. Vol. 66(2). p.185-93. DOI: https://doi.org/10.12989/sem.2018.66.2.185.

[12] Garcia-Palencia A, Santini-Bell E, Gul M, Catbas N. “A FRF-based algorithm for damage detection using experimentally collected data”. *Structural Monitoring and Maintenance*. December 2015. Vol. 2(4). p.399-418. DOI: http://dx.doi.org/10.12989/smm.2015.2.4.399.

[13] Sulaiman MS, Yunus MA, Bahari AR, Rani MA. “Identification of damage based on frequency response function (FRF) data”. *InMATEC Web of Conferences* 2017 (Vol. 90, p. 01025). EDP Sciences. DOI: https://doi.org/10.1051/matecconf/20179001025.

[14] Esfandiari A, Chaei MG, Rofooei FR. “A structural model updating method using incomplete power spectral density function and modal data”. *Structural engineering and mechanics*: *An international journal*. 2018. Vol.68(1). p.39-51. DOI: https://doi.org/10.12989/sem.2018.68.1.039.

[15] Sha G, Radzieński M, Cao M, Ostachowicz W. “A novel method for single and multiple damage detection in beams using relative natural frequency changes”. *Mechanical Systems and Signal Processing*. October 2019. p.132:335-52. DOI: https://doi.org/10.1016/j.ymssp.2019.06.027

[16] He K, Zhu WD. “Structural damage detection using changes in natural frequencies: theory and applications”. *InJournal of Physics: Conference Series* 2011 Jul 19 (Vol. 305, No. 1, p. 012054). IOP Publishing. DOI: https://doi.org/10.1088/1742-6596/305/1/012054

[17] Wickramasinghe WR, Thambiratnam DP, Chan TH. “Damage detection in a suspension bridge using modal flexibility method”. *Engineering failure analysis*. January 2020. Vol. 107. p.104194. DOI: https://doi.org/10.1016/j.engfailanal.2019.104194

[18] Liu K, Yan RJ, Soares CG. “Damage identification in offshore jacket structures based on modal flexibility”. *Ocean Engineering*. December 2018. Vol. 170. p.171-85. DOI: https://doi.org/10.1016/j.oceaneng.2018.10.014

[19] Yang D, Kang C, Hu Z, Ye B, Xiang P. “On the study of element modal strain energy sensitivity for damage detection of functionally graded beams”. *Composite Structures*. September 2019. Vol. 224. p.110989. DOI: https://doi.org/10.1016/j.compstruct.2019.110989

[20] Teng S, Chen G, Liu G, Lv J, Cui F. “Modal strain energy-based structural damage detection using convolutional neural networks”. *Applied Sciences.* January 2019. Vol. 9(16). p.3376. DOI: https://doi.org/10.3390/app9163376

[21] He WY, He J, Ren WX. “Damage localization of beam structures using mode shape extracted from moving vehicle response”. *Measurement.* June 2018 Vol. 121. p.276-85. DOI: https://doi.org/10.1016/j.measurement.2018.02.066

[22] Padil KH, Bakhary N, Abdulkareem M, Li J, Hao H. “Non-probabilistic method to consider uncertainties in frequency response function for vibration-based damage detection using artificial neural network”. *Journal of Sound and Vibration.* February 2020. Vol. 467. p.115069. DOI: https://doi.org/10.1016/j.jsv.2019.115069

[23] Bagherahmadi SA, Seyedpoor SM. “Structural damage detection using a damage probability index based on frequency response function and strain energy concept”. *Structural Engineering and Mechanics.* January 2018. Vol. 67(4). p.327-36. DOI: https://doi.org/10.12989/sem.2018.67.4.327.

[24] Barman SK, Mishra M, Maiti DK, Maity D. “Vibration-based damage detection of structures employing Bayesian data fusion coupled with TLBO optimization algorithm”. *Structural and Multidisciplinary Optimization*. October 2021. Vol. 64(4). p.2243-66. DOI: https://doi.org/10.1007/s00158-021-02980-6.

[25] Altunışık AC, Okur FY, Karaca S, Kahya V. “Vibration-based damage detection in beam structures with multiple cracks: modal curvature vs. modal flexibility methods”. *Non-destructive Testing and Evaluation*. January 2019. Vol.34(1). p.33-53. DOI: https://doi.org/10.1080/10589759.2018.1518445

[26] Rezvani K, Sabour MH. “A comparison of some methods for structural damage detection”. *Scientia Iranica*. June 2018. Vol. 25(3). p.1312-22. DOI: https://doi.org/10.24200/sci.2017.4494.

[27] Gomes HM, Silva NR. “Some comparisons for damage detection on structures using genetic algorithms and modal sensitivity method”. *Applied Mathematical Modelling*. November 2008. Vol. 32(11). p.2216-32. DOI: https://doi.org/10.1016/j.apm.2007.07.002.

[28] Kim YS, Eun HC. “Comparison of damage detection methods depending on frfs within specified frequency ranges”. *Advances in Materials Science and Engineering*. January 2017. DOI: https://doi.org/10.1155/2017/5821835.

[29] Esfandiari A, Bakhtiari-Nejad F, Sanayei M, Rahai A. “Structural finite element model updating using transfer function data”. *Computers & structures*. January 2010. Vol. 88(1-2). p.54-64. DOI: https://doi.org/10.1016/j.compstruc.2009.09.004.

[30] Vahedi M, Khoshnoudian F. “Sensitivity-based damage identification method for structures exposed to ground excitation”. *Inverse Problems in Science and Engineering*. October 2018. Vol.26(10). p.1404-31. DOI: https://doi.org/10.1080/17415977.2017.1406487

[31] Shadan F, Khoshnoudian F, Esfandiari A. “A frequency response-based structural damage identification using model updating method”. *Structural Control and Health Monitoring*. February 2016. Vol. 23(2). p.286-302. DOI: https://doi.org/10.1002/stc.1768

[32] Pedram M, Esfandiari A. “Mitigating the effect of incomplete measurement in sensitivity-based FE model updating by enhanced transfer function”. *Iranian Journal of Science and Technology*, *Transactions of Civil Engineering*. July 2019. Vol.43(1). p.467-86. DOI: https://doi.org/10.1007/s40996-018-0180-6.

[33] Zheng ZD, Lu ZR, Chen WH, Liu JK. “Structural damage identification based on power spectral density sensitivity analysis of dynamic responses”. *Computers & Structures*. January 2015. Vol. 146. p.176-84. DOI: https://doi.org/10.1016/j.compstruc.2014.10.011.

[34] Bayat1a M, Ahmadi HR, Mahdavi N. “Application of power spectral density function for damage diagnosis of bridge piers”. *Structural Engineering and Mechanics*. 2019. Vol. 71(1). p.57-63. DOI: https://doi.org/10.12989/sem.2019.71.1.057.

[35] Gunawan FE. “Reliability of the power spectral density method in predicting structural integrity”. *International journal of innovative computing*, information and control. 2019. Vol.15(5). p.1717-27. DOI: https://doi.org/10.24507/ijicic.15.05.1717.
[36] Pedram M, Esfandiari A, Khedmati MR. “Damage detection by a FE model updating method using power spectral density: Numerical and experimental investigation”. *Journal of Sound and Vibration*. June 2017. Vol. 397. p.51-76. DOI: https://doi.org/10.1016/j.jsv.2017.02.052.
[37] Pedram M, Esfandiari A, Khedmati MR. “Frequency domain damage detection of plate and shell structures by finite element model updating”. *Inverse Problems in Science and Engineering*. January 2018. Vol. 26(1). p.100-32. DOI: https://doi.org/10.1080/17415977.2017.1309398.
[38] Esfandiari A, Bakhtiari-Nejad F, Rahai A, Sanayei M. “Structural model updating using frequency response function and quasi-linear sensitivity equation”. *Journal of sound and vibration*. October 2009. Vol. 326(3-5). p.557-73. DOI: https://doi.org/10.1016/j.jsv.2009.07.001.
[39] Farshadi M, Esfandiari A, Vahedi M. “Structural model updating using incomplete transfer function and modal data”. *Structural Control and Health Monitoring*. July 2017. Vol. 24(7). p.e1932. DOI: https://doi.org/10.1002/stc.1932.

ISSN: 0012-7361 eISSN: 1989-1490 / DYNA Vol. 97 n.1 DOI: https://doi.org/10.6036/10504